Atarés Huerta, LM.; Depypere, F.; Pieters, J.; Dewettinck, K. (2012). Coating quality as affected by core particle segregation in fluidized bed processing. Journal of Food Engineering. 113(3):415-421. doi:10.1016/j.jfoodeng.2012.06.012

Elsevier Editorial System(tm) for Journal of Food Engineering
Manuscript Draft

Manuscript Number:

Title: COATING QUALITY AS AFFECTED BY CORE PARTICLE SEGREGATION IN FLUIDIZED BED PROCESSING

Article Type: Research Article

Keywords: food powder; fluidized bed coating; Confocal Laser Scanning Microscopy; Positron Emission Particle Tracking; coating quality

Corresponding Author: Ms Lorena Atares, Ph.D.

Corresponding Author's Institution: Universidad Politécnica de Valencia

First Author: Lorena Atares, Ph.D.

Order of Authors: Lorena Atares, Ph.D.; Frédéric Depypere, Dr.; Jan G Pieters, Prof; Koen Dewettinck, Prof

Abstract: Fluidized bed coating is an important technique in the food powder industry, where often particles of a wide size distribution are dealt with. In this paper, glass beads of different particle size distribution were coated with sodium caseinate in a top-spray fluid bed unit. Positron Emission Particle Tracking (PEPT) was used to visualize and quantify the particle motion in the fluidized bed. Confocal Laser Scanning Microscopy combined with image analysis were used to investigate the effect of core particle size and its distribution on the thickness and quality of the coating. Particle size significantly affected the thickness and quality of the coating, due to differences in the corresponding fluidization patterns, as corroborated by PEPT observations. As the particle size distribution becomes narrower, segregation is less likely to occur. This results in a thicker coating which is, however, less uniform compared to when cores of a wider particle size distribution are spray coated.

Cover Letter

INSTITUTO DE INGENIERÍA DE ALIMENTOS PARA EL DESARROLLO

UNIVERSIDAD POLITECNICA DE VALENCIA

R. Paul Singh

Professor of Food Engineering

Department of Biological and Agricultural Engineering

University of California

April 17th, 2012

Concerning: Papers submission for Journal of Food Engineering

Dear Prof. R.P. Singh,

please find with this submission the original research paper entitled "COATING QUALITY AS AFFECTED BY CORE PARTICLE SEGREGATION IN FLUIDIZED BED PROCESSING " which we would like to consider for publication in a same issue of the Journal of Food Engineering.

Hereby we provide you with the names and addresses of 3 potential reviewers (in alphabetical order):

Prof. Elisabeth Dumoulin, ENSIA, Department of Food Process Engineering, Massy Cedex, France.
E-mail: dumoulin@ensia.inra.fr
Prof. Gabrie Meesters, TU Delft, Department of Chemical Technology, Particle Technology Group, Julianalaan 136, 2628 BL Delft, The Netherlands
E-mail: Gabrie.Meesters@dsm.com
Prof. Denis Poncelet, ENITIAA, Rue de la Géraudière BP 8225, 44322 Nantes Cedex 3, France.
E-mail: poncelet@enitiaa-nantes.fr

Furthermore, we have no restrictions for other reviewers that could be contacted.

We hope to hereby have provided with sufficient information to consider this publication for the reviewing stage. If you would need more information, please do not hesitate to contact me (loathue@tal.upv.es).

With best regards,
Dr. Lorena Atarés
in name of the other co-authors (Dr. Frédéric Depypere, Prof. J.G. Pieters, Prof. K. Dewettinck)

***Highlights (for review)**

- CLSM is able to characterize microparticles and quantify the coating thickness.
- The thickness and quality of the coating was affected by the size of the particles
- PEPT findings supported these results
- Our results help understand particle motion patterns, coating thickness and quality

COATING QUALITY AS AFFECTED BY CORE PARTICLE SEGREGATION IN FLUIDIZED BED PROCESSING

L. Atarés [a,*], F. Depypere [b], J.G. Pieters [c], K. Dewettinck [b]

[a] Instituto Universitario de Ingeniería de Alimentos para el Desarrollo, Universitat Politècnica de València, Camino de Vera, s/n 46022 Valencia, Spain

[b] Department of Food Safety and Food Quality, Faculty of Bioscience Engineering, Ghent University, Coupure Links 653, 9000 Ghent, Belgium

c Department of Biosystems Engineering, Faculty of Bioscience Engineering, Ghent University, Coupure Links 653, 9000 Ghent, Belgium

ABSTRACT

Fluidized bed coating is an important technique in the food powder industry, where often particles of a wide size distribution are dealt with. In this paper, glass beads of different particle size distribution were coated with sodium caseinate in a top-spray fluid bed unit. Positron Emission Particle Tracking (PEPT) was used to visualize and quantify the particle motion in the fluidized bed. Confocal Laser Scanning Microscopy combined with image analysis were used to investigate the effect of core particle size and its distribution on the thickness and quality of the coating. Particle size significantly affected the thickness and quality of the coating, due to differences in the corresponding fluidization patterns, as corroborated by PEPT observations. As the particle size distribution becomes narrower, segregation is less likely to occur. This results in a thicker coating which is, however, less uniform compared to when cores of a wider particle size distribution are spray coated.

Key words: food powder, fluidized bed coating, Confocal Laser Scanning Microscopy, Positron Emission Particle Tracking, coating quality.

1. INTRODUCTION

Fluidized bed coating, traditionally utilised in the domain of pharmaceutical industries, has evolved to an important technique in food industry. This process enables to encapsulate solid microparticles (Risch & Reineccius, 1995) of sizes between 50 and 1000μm, which remain in suspension by an upward moving heated air stream entering the bed via the bottom of the reactor

* corresponding author: loathue@tal.upv.es

through an air distributor. The aqueous coating material is sprayed in the form of very small droplets of 10-40 μm (Vanderroost et al., 2011) by a nozzle placed above the fluidized bed working at a selected atomization air pressure. While travelling through the bed, both solid particles and coating material droplets exchange mass and heat with one another, with the air contained in the bed and with the reactor wall. As the process progresses, the coating solution repeatedly wets the surface of the solids and dries, which results in the coating of the core material.

A variety of core materials have been investigated in fluidization studies, such as sand, silica gel, alumina, limestone (Harris et al., 2003), or anhydrous sodium sulphate (Hede et al., 2007). More realistic food cores, such as sucrose/starch beads, have also been used (Depypere et al., 2009a). Glass has been frequently used as a model core material, which involves a significant simplification as opposed to real food powders. Glass microbeads are spherical, inert, non-porous and their size distribution is narrower than that of real food powders. Some examples of coating materials are maltodextrin (Ronsse et al., 2011), sodium caseinate and gelatin hydrolysate (Depypere et al., 2009a). In the latter study, it was found that the sodium caseinate solution spray and the resulting coating hardly influenced the motion patterns of the fluidized particles. This was not the case for gelatin hydrolysate, whose higher stickiness led to an overall slowed down solids particle motion.

According to Vanderroost et al. (2011), the quality of the coating process taking place in a fluidized bed is largely determined by the spray characteristics and the particle motion. Larsen et al. (2003) stated that the control of a coating process has been traditionally based on set points for the most critical process variables (spray rate, process airflow, nozzle atomizing airflow, inlet air temperature and humidity…) and the practical experience of the operator. If formulation or process conditions are incorrectly chosen, a poor product quality will be the result (Hede et al., 2007). Previous studies have aimed to contribute to the understanding of how these factors affect the particle motion in the reactor (Depypere et al., 2009a) but, to the best of our knowledge, there are no studies reported in which the relationship with the final quality of the coating on the solid particles has been described.

For the purpose of particle coating process control, the measurement of the coating thickness is needed. If the coating is too thin, it will not succeed in its required performance (controlled release, protection of the core material…), and if it is too thick delayed release will result, as well as increased coating process times and increased costs (Andersson et al., 1999). The quality of the coating film can be assessed by the combined use of Confocal Laser Scanning Microscopy (CLSM) and image

analysis. CLSM has proved its usefulness in food science (Dürrenberger et al., 2001). This microscopy technique forms a bridge between light and electron microscopy, displaying a high magnifying power and no need for extensive sample preparation, as samples can be observed in their natural state. CLSM allows the operator to optically section the microparticle at any desired plane, through exclusion of fluorescence emitted from any region of the sample other than the focal plane under study. Moreover, the core and the coating materials can be distinguished on the basis of a difference in fluorescence intensity (Anderson et al., 2000). The combination of CLSM with computational image analysis allows for the quantification of the coating thickness (Lamprecht et al., 2000). However, an average coating thickness on itself may not adequately characterize a population of coated microparticles. Some other important data to characterize the quality of the coating are the intra-particle and inter-particle coating variability, the coating uniformity and the presence of coating deficiencies (Depypere et al., 2009b).

This work aimed to assess the coating thickness and quality of glass microparticles produced by fluidized bed coating, based on the use of CLSM and image analysis. Experiments were set up in which the width of the core particle size distribution was varied and Positron Emission Particle Tracking experiments were performed to assess the resulting particle motion in the tapered fluid bed. The extent of particle segregation during fluid bed processing was tested for its influence on the coating thickness and quality.

2. MATERIALS AND METHODS

2.1. Core and coating materials

Spherical glass beads (Microbeads®, Sovitec, Belgium) of three different size ranges (named AF, AC and C) were used as core material for the top-spray fluidized bed coating experiments. Their general properties (average diameters, density and shape) are reported in Table 1. The particle size distribution of the investigated powders was measured with a laser diffraction device (Mastersizer S) equipped with a MSX-64 Dry Powder Feeder (Malvern, United Kingdom), a 300 mm lens (0.5-900 μm) and a 1000 mm lens (4-3500 μm). Both a surface weighted average diameter (d_{32}) and a volume weighted average diameter (d_{43}) were calculated based on 10 replicates. Particle density (ρ_p) was

measured via toluene pycnometry at 25°C (5 replicates) and particle shape was analysed using a Leitz Diaplan light microscope equipped with a Nikon Coolpix 4500 digital camera.

A sodium caseinate aqueous solution (10%w/w) was used as coating material. The protein was provided by Armor protein (France). The coating solution was prepared by staining demineralised water with 3 ppm Rhodamine B (Acros Organics, Belgium) prior to dispersing the protein. Rhodamine B is perfectly soluble in water and allows for further observation by CLSM. The mass of sodium caseinate required for each experiment was calculated with equation 1 (Dewettinck et al., 1998; Depypere et al., 2009b), aiming for a 5 μm coating thickness (d_c) in glass beads AC, assuming that the average radius of the core particle (r_p) is 100 μm and coating losses do not occur:

$$d_c = r_p \cdot \left(\left(1 + \frac{\rho_p \cdot M_c}{\rho_c \cdot M_p} \right)^{1/3} - 1 \right) \qquad \text{(eq.1)}$$

where M_c and M_p are the mass of coating dry matter and fluidized powder (kg), respectively, ρ_p is the particle density of the core particles (kg/m^3) and ρ_c is the density of the coating material (944 kg/m^3), which was obtained through toluene pycnometry.

2.2. Fluidized bed coating experiments

A laboratory-scale fluidized bed (Glatt GPCG-1, Glatt GmbH, Germany) with a tapered stainless steel vessel (560mm height, 8.1° inclination) and a steel woven wire mesh distributor was used for all the experiments. The diameters of the distributor and upper section of the chamber were 140 and 300mm, respectively. The nozzle was installed at 121 mm above the distributor. A more detailed description of the equipment can be found in Depypere et al. (2005). The temperature of the fluidisation air entering the system was set at 75°C, and 750g of bulk material (either glass beads AC or a 33% w/w mixture of glass beads AF/AC/C) was introduced into the bed. The filter on top of the reactor was automatically shaken to introduce solid particles back to the fluidized bed. A vane probe (Testo, Belgium) was used to measure the air flow rate inside the system. Every experiment was performed at 81 m^3/h air flow rate, corresponding to a superficial air velocity across the distributor of 1.5 m/s. The relative humidity or the inlet air was 61% (± 1%) in all experiments. The solution was pumped to the system at 5 g/min. An atomisation pressure of 3 bar was selected to operate the two-fluid nozzle (Zweistoffdüse Modell 970/S0, Düsen-Schlick, Germany).

2.3. CLSM procedure

The CLSM images of the coated glass beads were obtained with a Bio-Rad Radiance 2000 confocal laser scanning microscopy system (Bio-Rad, United Kingdom), attached to a Nikon Eclipse TE300 inverted fluorescence microscope (Bio-Rad, UK). A He/Ne-laser with a laser power of 1.4 mW, generating a green excitation line of 543 nm was used. Rhodamine B, originating from the coating,was detected on a photomultiplier using a HQ590/70 filter. All confocal images were taken with a Nikon S Fluor 40x objective (oil immersion, NA 1.30). This lens was operated at a working distance of 0.22 mm. All settings for the confocal microscope and the imaging of the microparticles were computer controlled through the software Lasersharp 2000 version 5.2 (Bio-Rad, UK). The following settings were used: laser power (30% of the maximum power), scan speed (500 lines per second), iris (6.0), gain (5.4) and offset (1.0).

A small amount of coated particles was dispersed in immersion oil (Merck, Germany, refractive index: 1.515) on a cover glass. As the refraction index of the glass beads and the immersion oil were identical, spherical aberration problems were minimised. The objective lens, located below the sample, was covered with immersion oil and was allowed to approach the bottom of the cover glass, until the sample was in focus. Upon changing the position of the focus motor, a sample was scanned in the vertical direction (viewing axis or z-axis).

Only images of the equatorial slice of glass beads were recorded. Through the selection of appropriate CLSM settings, as defined above, it was assured that the image was neither undersaturated nor oversaturated, as this would lead to the underestimation or the overestimation of the coating thickness, respectively. Using a 40x magnification lens, the confocal image covered an area of 272.9 x 272.9 μm^2. Given that digital image files of 512 x 512 pixel resolution were recorded, the area of the pixel was about 0.533x0.533 μm^2, and using this conversion factor, the actual thickness of the coatings could be calculated.

2.4. Image analysis, coating quality assessment and statistical analysis

Figure 1 briefly describes the protocol followed to obtain the raw coating thickness data from the CLSM images of the coated glass beads. Image analysis of the digital recordings was performed using the software Image J 1.32j (National Institutes of Health, USA), following the protocol described

by Depypere et al. (2009b). For every single glass bead, a distribution of coating thicknesses, corresponding to the 360 values obtained every degree around the perimeter of the spherical core particle, was acquired. From this distribution, three parameters were derived to describe the coating of that microparticle: the average coating thickness $d_{c,avg}$ (measure of the overall coating content), the standard deviation of the coating thickness distribution $d_{c,stdev}$ (measure of the coating heterogeneity) and the minimal value $d_{c,min}$ (measure of the occurrence of imperfections). Additionally, the coating quality of an individual coated glass bead was defined as the ratio of the average coating thickness ($d_{c,avg}$) to the standard deviation of the coating thickness distribution ($d_{c,stdev}$). The higher this ratio, i.e., the thicker a coating of equal homogeneity is, or the more homogeneous the coating thickness distribution around a same average value is, the better the coating quality (Depypere et al., 2009b).

To analyze the effect of different factors on the coating quality of glass beads, a number of microparticles from each experiment, representative of the bulk population, had to be investigated. In accordance with Depypere et al. (2009b), analysing 50 microparticles per batch proved to be adequate. Once the four parameters listed above were obtained from each individual particle, these were averaged over the random factor “particle”. To find whether these parameters differed significantly between different experiments, analysis of variance (ANOVA) tests were performed using Statgraphics Plus (Manugistics Corp., Rockville, MD). Fisher’s least significant difference (LSD) procedure was used.

2.5. Positron Emission Particle Tracking (PEPT) protocol

Positron Emission Particle Tracking (PEPT) is one of the few available non-invasive methods able to visualize and quantify the particle motion in real equipment. A single tracer was labeled with a radioisotope (fluorine-18) and introduced into the system. Upon decay of this radioisotope, positrons are released which annihilate with neighbouring electrons and hereby produce a pair of back-to-back γ-rays. By detecting multiple successive γ-ray pairs the tracer can be located with high spatial and temporal resolution using triangulation. The PEPT technique is described more in detail by Parker et al (1993, 2002). For glass beads belonging to a specific particle size, a single particle with hydrodynamic characteristics representative of the bulk material, i.e., with a mean particle size, was selected from the bulk powder and activated through surface adsorption (Depypere et al., 2009a).

177 The fluid bed device was positioned between the two camera detectors, having a useful cross
178 sectional area of 500 x 400mm^2 and separated from each other by 609 mm. The region of interest –
179 the product container and the expansion chamber – was situated within the borders of the detection
180 window. In a first test with the mixture of AF/AC/C core particles, the motion of a tracer particle
181 representative of the AF fraction was followed, while in the second test, a big (C) particle was selected
182 as the tracer. Finally, it was also tested whether segregation occurred between small and large
183 particles belonging to a same grade of glass beads.
184 Depypere et al. (2009a) also described in more details techniques used to extract further
185 quantitative information from the tracer location data: the expanded bed height, the total circulation
186 time (τ) and the frequencies of particles entering a specific zone. Based on the expanded bed height,
187 the powder bed was divided into three parts: a bottom-section extending from the bottom to 25% of
188 the bed height, a central section between 25% and 75% of the bed height and a top-section above
189 75% of the bed height, including the freeboard region. The total circulation time was defined as the
190 sum of: (1) the time the tracer spends in the bottom-section, (2) the time during which the tracer
191 moves from the bottom-section to the top-section, (3) the time spent in the top-section and (4) the
192 down-flow time between the top-section and the bottom-section. As Depypere et al. (2009a) found that
193 a lot of tracer revolutions did not follow the adopted definition of a circulation, they also introduced the
194 mean time between two successive circulations, $t_{c\text{-}c}$. In general the latter was found to be about twice
195 the value of the total mean particle circulation time.
196
197
198 **3. RESULTS AND DISCUSSION**
199
200 **3.1. Effect of the particle size on the coating thickness and quality**
201 A first experiment was performed where a mixture of glass beads of different sizes (AF, AC
202 and C, 33% w/w each) were coated with a sodium caseinate solution, sprayed at 3 bar atomization
203 pressure. After the coating experiment, for each particle size range, CLSM recordings of 50 glass

beads were considered in order to obtain the final results of $d_{c,avg}$, $d_{c,stdev}$, $d_{c,min}$ and coating quality. The average values and standard deviations of these results are represented in Figure 2. The results of average coating thickness are coherent to those found by Depypere et al. (2009b), when working with AC glass beads and sodium caseinate coatings of increased thickness.

In a mixture of glass beads of different grades, the core particle size had a statistically significant effect on all four coating parameters considered ($p<0.05$). It was confirmed that the targeted average coating thickness ($d_{c.avg}$), i.e. 5 μm, for AC beads was achieved, whereas it was significantly higher for AF particles and lower for C particles ($p<0.05$). Figure 3 represents the accumulated frequency of coating thickness for all 50 glass beads of each size range, where the same trend – the bigger the particles, the thinner the coating – can be observed.

Under the hypothesis that, in the fluid bed recognized for its excellent mixing capacity, segregation based on the particle size would not occur, all core particles would have an equal probability to pass through the coating zone of the spray nozzle. Taking into account the differences in specific area of the differently sized spherical particles, 250g of AF particles accounts for 53% of the total core surface area. The same mass of AC particles and C particles accounts for 30% and for 17%, respectively, of the total core surface area. Under the assumption that the coating would be evenly distributed per unit core particle surface area, and taking into account equation 1, the theoretical coating thicknesses would then be 4.24μm, 4.38 μm and 4.46 μm for AF, AC and C glass beads, respectively.

In practice, using equation 1, and considering the average $d_{c,avg}$ per size (Figure 2), we found that the mass of protein was indeed unevenly distributed among the different sizes: 61% of the protein coated AF particles, 26% coated AC particles and only 13% coated C particles. Based on the results shown in Figure 2 and the fact that, in practice, more coating material was retrieved on the smallest particles (AF) while less coating material was retrieved on the medium-sized (AC) and largest (C) particles, the initial hypothesis cannot be maintained and it was assumed that segregation based on the particle size occurred in the fluidized bed.

Figure 4 shows the combined occupancy and velocity vector plots in the XY-centre plane (data averaged over a thickness of 20 mm) for two successive PEPT experiments, in which a small and a big tracer, respectively, were used to follow the motion of a 750g mixture of 33 wt% of glass beads AF, AC and C, fluidised at Q = 81 m^3/h. It can be clearly observed that radial segregation in the

lower part of the bed took place: here the small particle tended to occupy an annular region close to the wall in preference to the core; the opposite is true for the large particle. In order to quantify the radial segregation, the normalised 1D-occupancy was plotted against bed height (Figure 5) for 2 radial sections: core (20 mm radius around the vertical axis) versus annular section. The extent of radial segregation is clearly demonstrated in Figure 6. While the big particle predominantly occupied the core, the smaller one predominantly occupied the annulus in the lower region of the bed. Furthermore, a small difference can be seen in the powder bed height: 115 mm for the large tracer; 125 mm for the small tracer. So, in addition to radial segregation, axial segregation due to size difference occurred, albeit to a smaller extent.

Thirdly, it can be observed from the velocity vector plots that the circulation of the smaller particle proceeded faster than that of the bigger particle. The total circulation time was quantified as 0.75 s and 1.08 s for the small and the big particle, respectively (Figure 6). This statistically significant ($p<0.001$) difference in circulation time was particularly noticeable for τ(up) and τ(down), which were considerably larger when a big particle was used as the tracer. Corresponding values for $t_{c\text{-}c}$, the mean time between two successive circulations, were 1.57 s and 2.38 s for the small and the big particle, respectively.

Our findings are in accordance with other segregation studies of a dry pharmaceutical granulate (with a continuous, bimodal particle size distribution), fluidised in a bench-scale conical fluidised bed. In their work, Wormsbecker et al. (2005) showed that the largest granules tend to accumulate at the centre bottom of the conical fluid bed.

Finally, it was also tested whether segregation occurred between small and large particles belonging to a same grade of glass beads. As the 1D-occupancy lines for the small and large tracer particle nearly coincided (results not shown), it could be concluded that within one single grade of glass beads, segregation in the tapered vessel of the GPCG-1 fluidised bed did not occur under the given circumstances.

3.2. Effect of particle size distribution on coating thickness and quality

The different fluidization patterns for different core sizes may explain the worse quality of big particles as compared to small, as represented in Figure 2. The average standard deviation of the coating thickness distributions ($d_{c,stdev}$), significantly increased as the beads size was increased

(p<0.05), which points out the worsening of the uniformity of the coating as the particle size was increased. Accordingly, the minimum coating thickness ($d_{c,min}$) showed a significant reduction as the particle size was increased (p<0.05). The occurrence of non-coated areas was quantified through the frequency (percentage) of glass beads presenting uncoated areas. These percentages were 2, 42 and 60% for AF, AC and C glass beads, respectively. Being heavier than the smaller particles, big particles could not easily reach the top of the fluidized bed, which is also the drier zone. Besides, they spent longer times moving downwards and through the bottom area, as compared to small. This motion pattern negatively affected the quality, for contact between particles is more likely to happen in these situations, hindering the proper drying of the coating solution and affecting the homogeneity of the coating.

The effect of the width of the particle size distribution on the coating properties was analysed by comparing the coating of AC particles in the experiment described above (section 3.1.) with a second experiment performed at the same atomization pressure (3 bar) where only AC glass beads were coated. The results of both experiments are reported in Table 2. It was found that the average coating thickness ($d_{c,avg}$) was significantly higher (p<0.05) when only AC particles were used as core material. As already commented, when the core mixture was coated, the protein distributed unevenly between the three particle size ranges and only 26% of the total protein (compared to the expected 30%) constituted the coating of AC particles at the end of the experiment. As the particle size distribution becomes narrower, segregation is less likely to occur. Now, fewer smaller particles accounting – in relative terms – for more coating coverage, are present, and more protein is available to coat the core particles whose size is close to 200µm. The effect of the particle size distribution on the coating thickness is also represented in Figure 7 through the cumulative coating thickness frequency considering all 50 glass beads of both populations, where the increased value of $d_{c,avg}$ as the distribution is narrowed can be observed.

The standard deviation of the coating thickness ($d_{c,stdev}$) was also significantly larger (p<0.05) when the particle size distribution was narrow, suggesting less uniformity in the coating thickness. Taking into account the increase of both $d_{c,avg}$ and $d_{c,stdev}$ as the particle size distribution becomes narrower, this factor did not have a significant effect on the coating quality (p>0.05), nor on the minimum coating thickness and the percentage of glass beads with uncoated areas.

4. CONCLUSIONS

CLSM was acknowledged as a very powerful technique for the characterization of microparticles and the quantification of coating thickness. In a segregation experiment, the thickness and quality of the coating was significantly affected by the size of the particles, with the larger cores being enveloped by thinner and less uniforms coatings while thicker and more uniform coatings were found around smaller core particles. These results were supported by PEPT findings, given that small particles were found to rise higher in the powder bed and move faster, as compared to bigger particles. With cores of a more narrow particle size distribution, segregation was found less likely to occur. Thicker, but less uniform, coatings were obtained compared to when cores of a wider particle size distribution are spray coated. Generally, the results reported in this paper provide important information to understand how core size and particle motion patterns affect the coating thickness and quality.

5. ACKNOWLEDGEMENTS

The authors wish to thank the financial support received from the Fund for Scientific Research-Flanders (Belgium) (F.W.O.-Vlaanderen), as well as from the *Programa de Apoyo a la Investigación y Desarrollo* from the *Universitat Politècnica de València*.

6. REFERENCES

Andersson, M., Josefson, M., Langkilde, F.W., & Wahlund, K.G. (1999). Monitoring of a film coating process for tablet using near infrared reflectance spectroscopy. J. Pharmaceut. Biomed. Anal. 20 (1-2) 27-37.

Andersson, M., Holmquist, B., Lindquist, J., Nilsson, O., Wahlund, K.G. (2000). Analysis of film coating thickness and surface area of pharmaceutical pellets using fluorescence microscopy and image analysis, J. Pharmaceut. Biomed. Anal. 22 (2) 325–339.

Depypere, F., Pieters, J.G., & Dewettinck, K. (2005). Expanded bed height determination in a tapered fluidised bed reactor. *Journal of Food Engineering* 67, 353-359.

Depypere, F., Van Oostveldt, P., Pieters, J.G., & Dewettinck, K. (2009a). PEPT visualisation of particle motion in a tapered fluidised bed coater. *Journal of Food Engineering* 93, 324-336.

Depypere, F., Van Oostveldt, P., Pieters, J.G., & Dewettinck, K. (2009b). Quantification of microparticle coating quality by confocal laser scaning microscopy (CLSM). *European Journal of Pharmaceutics and Biopharmaceutics* 73, 179-186.

Dewettinck, K., & Huyghebaert, A., (1998). Top-spray fluidized bed coating: effect of process variables on coating efficiency. Lebensmittel-Wissenschaft und – Technologie – Food Science and Technology 31 (6), 568–575.

Dewettinck, K., Deroo, L., Messens, W., & Huyghebaert, A. (1998). Agglomeration tendency during top-spray fluidized bed coating with gums. Lebensmittel-Wissenschaft und – Technologie – Food Sci. Technol. 31 (6), 576–584.

Dürrenberger, M.B., Handschin, S., Conde-Petit, B., & Escher, F. (2001). Visualization of Food Structure by Confocal Laser Scanning Microscopy (CLSM). Lebensm. Wiss. U. Technol., 34, 11-17.

Harris, A.T., Davidson, J.F., & Thorpe, R.B. (2003). Particle residence time distributions in circulating fluidised beds. *Chemical Engineering Science* 58, 2181-2202.

Hede, P.D., Bach, P., & Jensen, A.D. (2007). Small-scale top-spray fluidized bed coating: granule impact strength, agglomeration tendency and coating layer morphology.

Lamprecht, A., Schäfer, U., & Lehr,C.M. (2000). Visualization and quantification of polymer distribution in microcapsules by confocal laser scanning microscopy, *Int. J. Pharmaceut*. 196 (2) (2000) 223–226.

Larsen, C.C., Sonnergaard, J.M., Bertelsen, P., & Holm, P. (2003). A new process control strategy for aqueous film coating of pellets in fluidized bed. *European Journal of Pharmaceutical Sciences* 20, 273-283.

Parker, D.J., Broadbent, C.J., Fowles, P., Hawkesworth, M.R., & McNeil, P.A., (1993). Positron emission particle tracking – a technique for studying flow within engineering equipment. *Nuclear Instruments and Methods in Physics Research* A 326 (3), 592–607.

Parker, D.J., Forster, R.N., Fowles, P., & Takhar, P.S., (2002). Positron emission particle tracking using the new Birmingham positron camera. *Nuclear Instruments and Methods in Physics Research* A 477 (1–3), 540–545.

Risch, S.J., Reineccius, G.A., (1995). Encapsulation and controlled release of food ingredients, ACS Symposium Series 590, Washington DC.

354 Ronsse, F., Depelchin, J., & Pieters, J.G. (2011). Particle surface moisture content estimation using
355 population balance modelling in fluidised bed agglomeration. *Journal of Food Engineering (in*
356 *press)*
357 Vanderroost, M., Ronsse, F., Dewettinck, K., & Pieters, J. (2011). Modelling coating quality in fluidized
358 bed coating: Spray sub-model. *Journal of Food Engineering* 106, 220-227.
359 Wormsbecker, M., Adams, A., Pugsley, T., & Winters, C. (2005). Segregation by size difference in a
360 conical fluidized bed of pharmaceutical granulate. *Powder Technology* 153 (1), 72-80.
361

Figure Captions

Figure 1: CLSM image segmentation and further processing protocol

Figure 2: Effect of the glass beads size on the average coating thickness ($d_{c,avg}$), average standard deviation of the coating thickness distributions ($d_{c,stdev}$), minimum coating thickness ($d_{c,min}$) and coating quality. CLSM coating thickness distribution data of 50 individual microparticles per test. A different superscript letter indicates significantly different values ($p<0.05$).

Figure 3: Effect of the glass bead size on the accumulated frequency of coating thickness (50 glass beads per size range)

Figure 4: Fluidisation of a 33 wt% glass beads AF/AC/C mixture with a small (left) and big (right) particle as a tracer (Q = 81 m^3/h).

Figure 5. Fluidisation of a 33 wt% glass beads AF/AC/C mixture with a small and big particle as a tracer (Q = 81 m^3/h): influence of particle size on total mean circulation time, τ, its breakdown, and the mean time between two subsequent circulations, t_{c-c} (●).

Figure 6: Fluidisation of a 33 wt% glass beads AF/AC/C mixture: 1-D occupancy of the big (circles) and small (squares) particles in the core (closed symbols) and annulus (open symbols).

Figure 7: Effect of the width of the particle size distribution on the accumulated frequency of coating thickness of AC glass beads (50 beads per experiment)

Figure 1

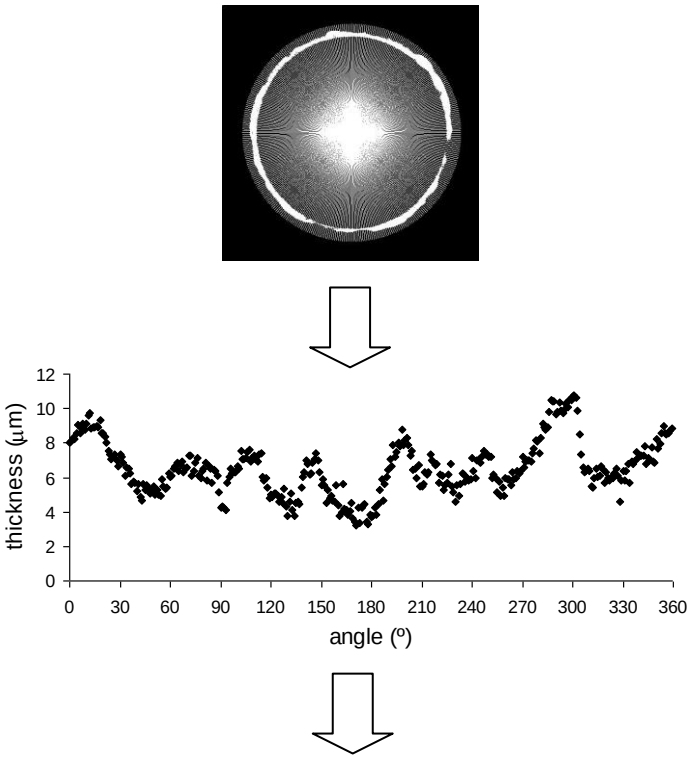

Individual parameters:

- coating thickness ($d_{c,avg}$)
- standard deviation ($d_{c,stdev}$)
- minimum coating thickness ($d_{c,min}$)
- coating quality

Figure 2

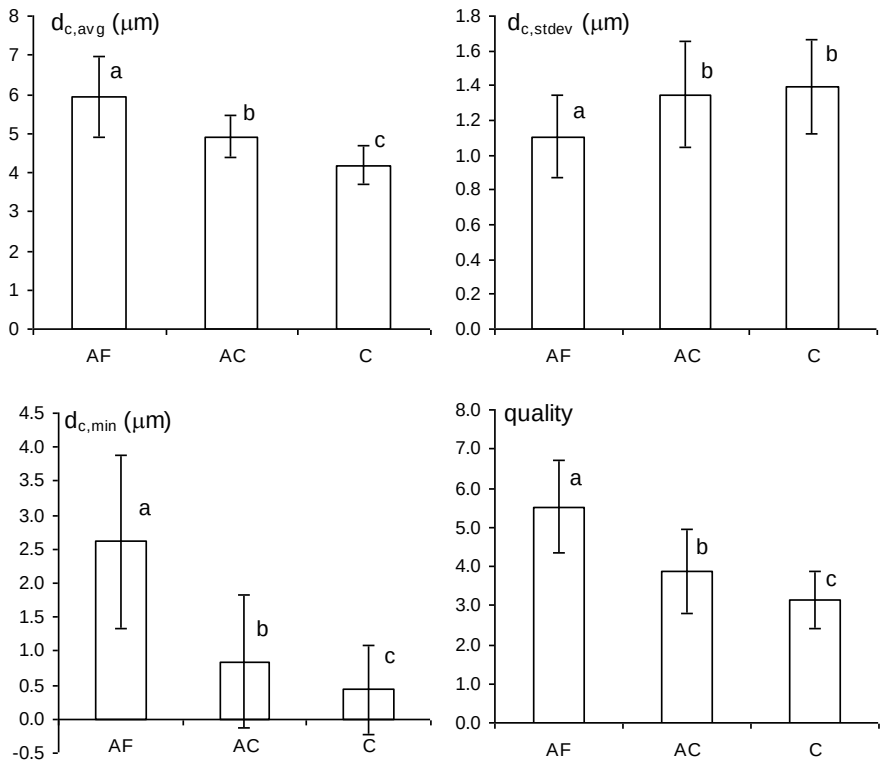
$d_{c,avg}$ (μm)
a
b
c
AF
AC
C
$d_{c,stdev}$ (μm)
a
b
b
AF
AC
C
$d_{c,min}$ (μm)
a
b
c
AF
AC
C
quality
a
b
c
AF
AC
C

Figure 3

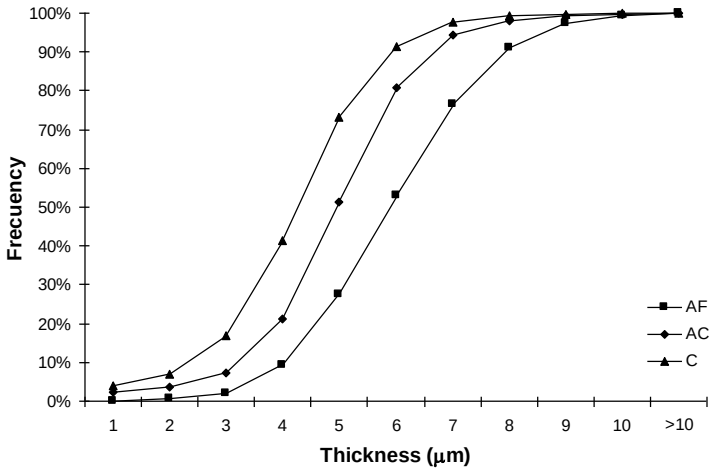
100%
90%
80%
70%
60%
50%
40%
30%
20%
10%
0%
Frecuency
1
2
3
4
5
6
7
8
9
10
>10
Thickness (μm)
AF
AC
C

Figure 4

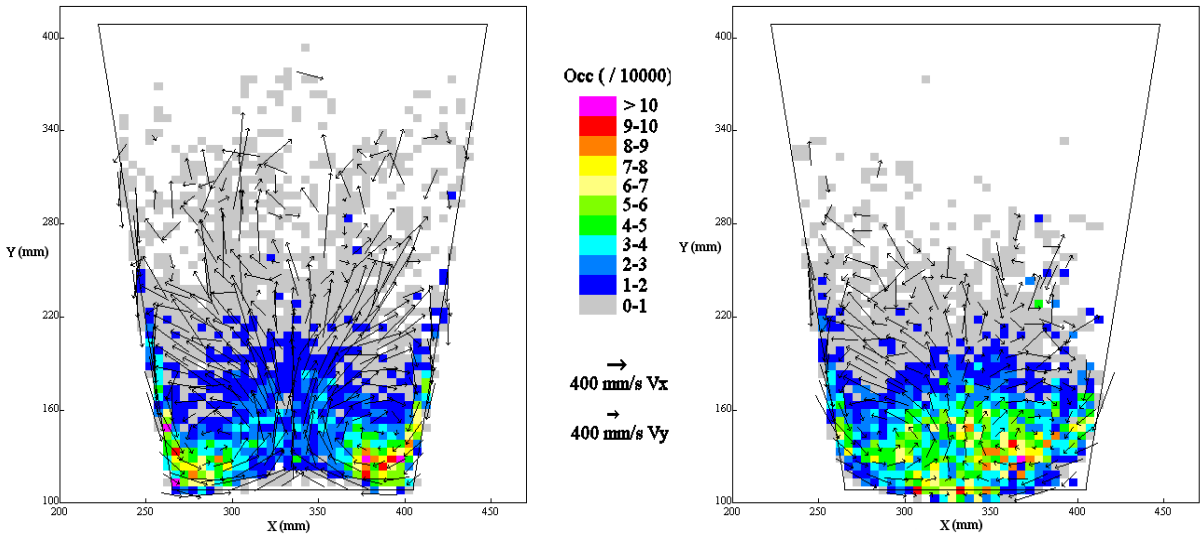
Y (mm)
X (mm)
Occ (/ 10000)
> 10
9-10
8-9
7-8
6-7
5-6
4-5
3-4
2-3
1-2
0-1
400 mm/s Vx
400 mm/s Vy

Figure 5

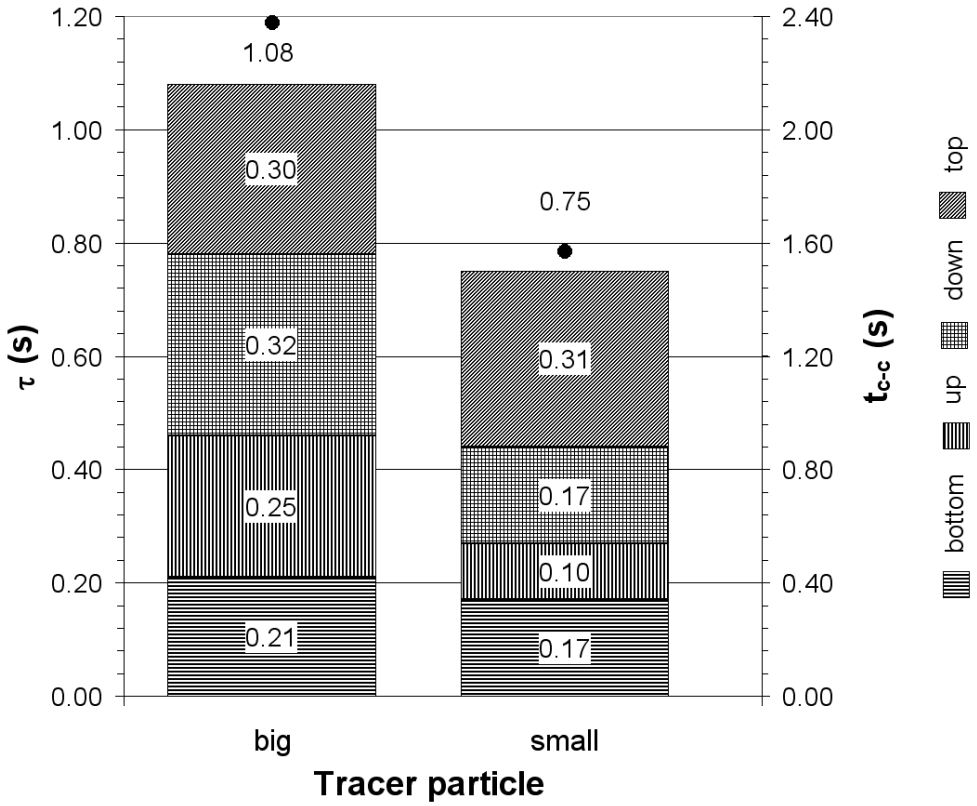
1.20
1.00
0.80
0.60
0.40
0.20
0.00
τ (s)
2.40
2.00
1.60
1.20
0.80
0.40
0.00
t_{c-c} (s)
1.08
0.75
0.30
0.32
0.25
0.21
0.31
0.17
0.10
0.17
top
down
up
bottom
big
small
Tracer particle

Figure 6

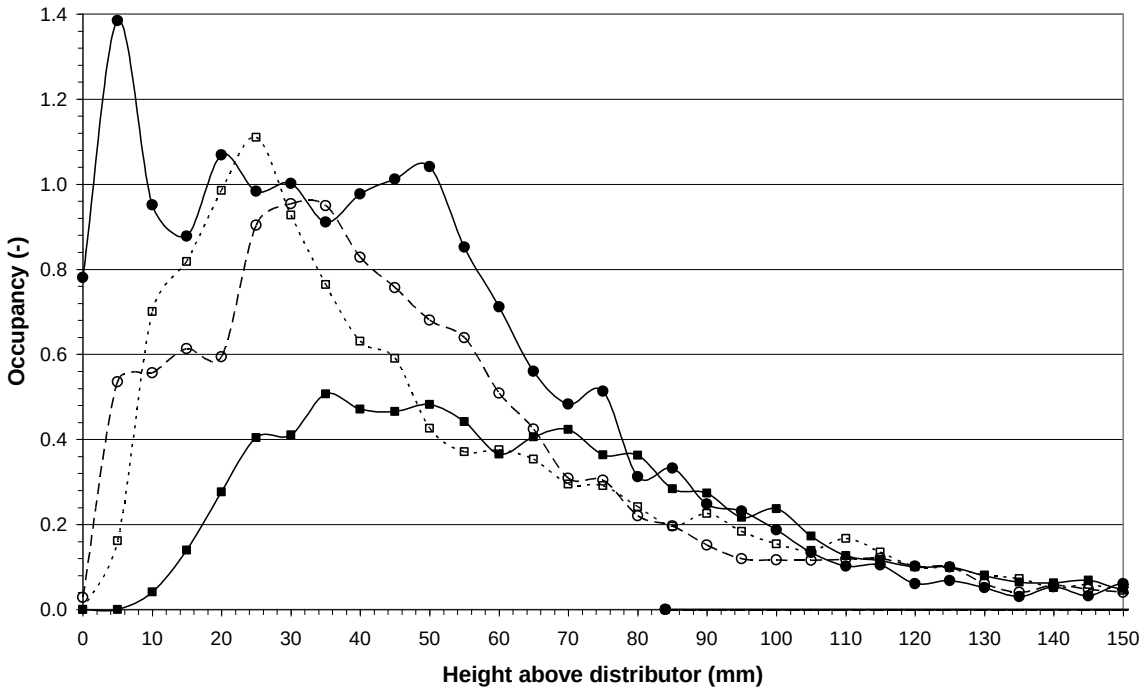
Occupancy (-)
1.4
1.2
1.0
0.8
0.6
0.4
0.2
0.0
0
10
20
30
40
50
60
70
80
90
100
110
120
130
140
150
Height above distributor (mm)

Figure 7

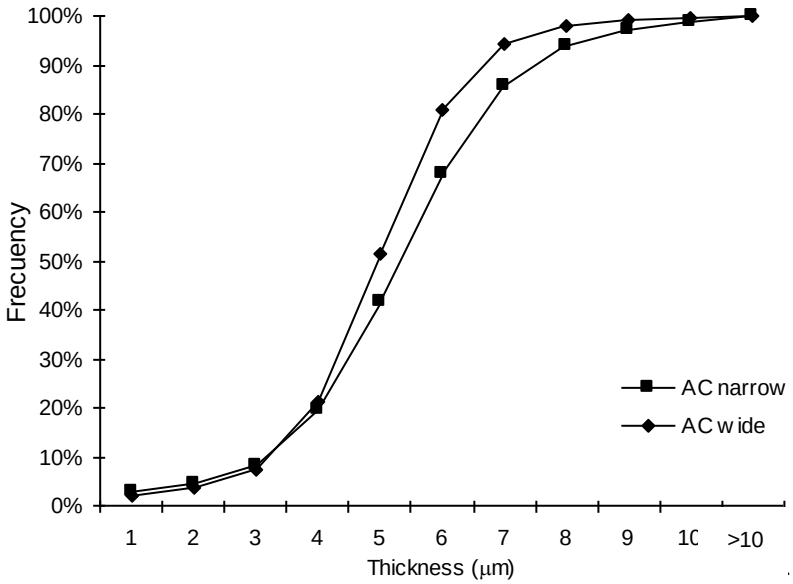
100%
90%
80%
70%
60%
50%
40%
30%
20%
10%
0%
Frecuency
1
2
3
4
5
6
7
8
9
10
>10
Thickness (μm)
AC narrow
AC w ide

Tables captions

Table 1: Average diameters, density and shape of core materials (average values and standard deviations in brackets)

Table 2: Effect of the width of the size distribution on the average coating thickness ($d_{c,avg}$), average standard deviation of the coating thickness distributions ($d_{c,stdev}$), minimum coating thickness ($d_{c,min}$) and coating quality of AC glass beads. CLSM coating thickness distribution data of 50 individual microparticles per test. A different superscript letter (^{xy}) indicates significantly different values ($p<0.05$).

Table 1

Glass beads	d_{32} (μm)	d_{43} (μm)	density (kg/m^3)
AF	108.69 (0.06)	110.93 (0.06)	2463 (6)
AC	196.54 (0.64)	204.18 (0.56)	2467 (3)
C	338.00 (0.75)	354.64 (0.71)	2481 (8)
AF/AC/C (33% w/w each)	176.81 (1.77)	234.76 (2.27)	2470 (3)

Table 2

Size distribution	wide	narrow
$d_{c,avg}$ (μm)	4.92 (0.53)[x]	5.30 (0.79)[y]
$d_{c,stdev}$ (μm)	1.35 (0.30)[x]	1.62 (0.41)[y]
$d_{c,min}$ (μm)	0.85 (0.99)[x]	1.06 (1.21)[x]
% beads with uncoated areas	42%	42%
Coating quality	3.86 (1.08)[x]	3.49 (1.01)[x]